

2018

Cosmic Ray Muons in the Standard Model of Fundamental Particles

Angel Gutarra-Leon

George Mason University, agutarr2@masonlive.gmu.edu

Cioli Barazandeh

Northern Virginia Community College

Walerian Majewski

Northern Virginia Community College, walerus@aol.com

Follow this and additional works at: <https://commons.vccs.edu/exigence>



Part of the [Elementary Particles and Fields and String Theory Commons](#)

Recommended Citation

Gutarra-Leon, A., Barazandeh, C., & Majewski, W. (2018). Cosmic Ray Muons in the Standard Model of Fundamental Particles. *Exigence*, 2 (1). <http://dx.doi.org/1082>

This Article is brought to you for free and open access by Digital Commons @ VCCS. It has been accepted for inclusion in Exigence by an authorized editor of Digital Commons @ VCCS. For more information, please contact tcassidy@vccs.edu.

Cosmic Ray Muons in the Standard Model of Fundamental Particles

Cover Page Footnote

We would like to thank the Society of Physics Students and the NVCC Educational Foundation for their generous grant support, and the Thomas Jefferson National Accelerator Facility in Newport News, VA for the donation of our scintillator.

Introduction

Muons (denoted by μ) are leptons, fundamental particles that also include electrons (denoted by e), tau-particles and their three neutrinos (denoted by ν , with a respective subscript), which cannot be subdivided. They are not subject to the nuclear-strength interaction. Muons are constantly being created by cosmic-ray high-energy protons, which collide with nuclei of the upper atmosphere where they produce showers of unstable non-elementary pions, which in turn decay into muons. The muon is like electron but is 200 times heavier and is thus itself unstable. It decays in microseconds (10^{-6} s) into three new particles: an electron, an electron antineutrino and a muon neutrino. (Physics Open Lab).

Figure 1. Artistic rendering of the muon production by cosmic rays in the atmosphere

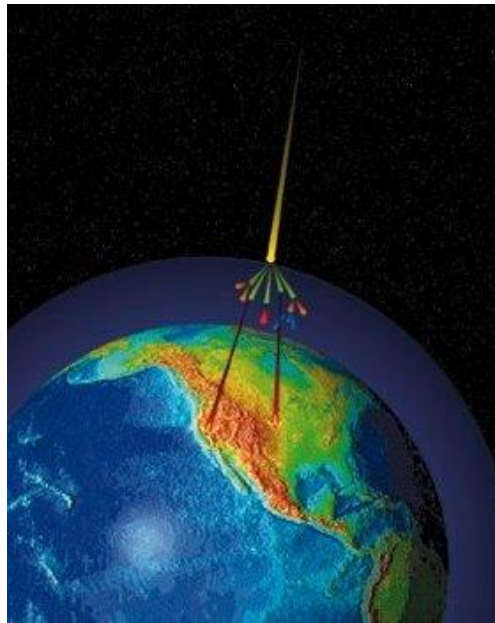


Figure 2. Rendering of pion creation and subsequent decay into a muon and a neutrino.

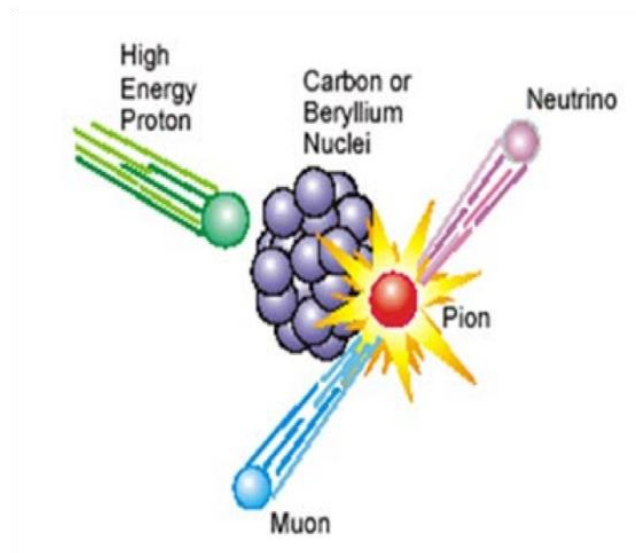


Figure 3. Diagram of the muon creation and decay into an electron and neutrinos

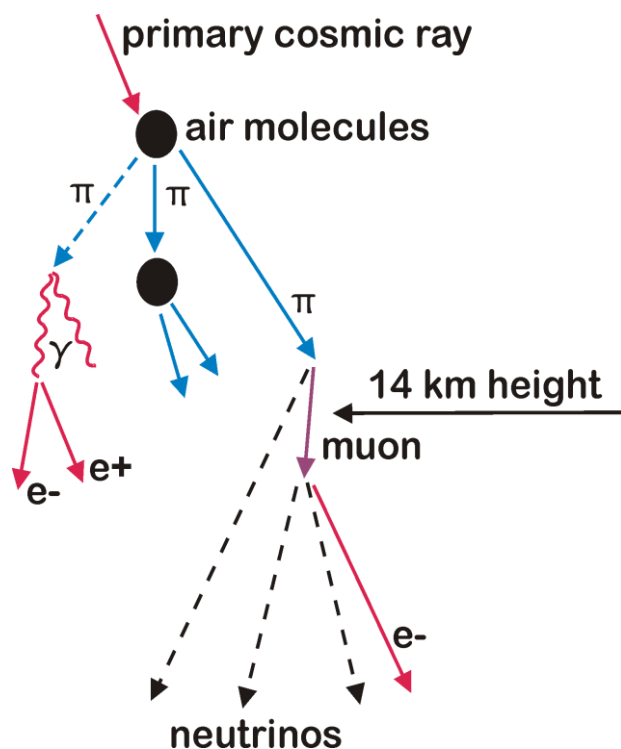
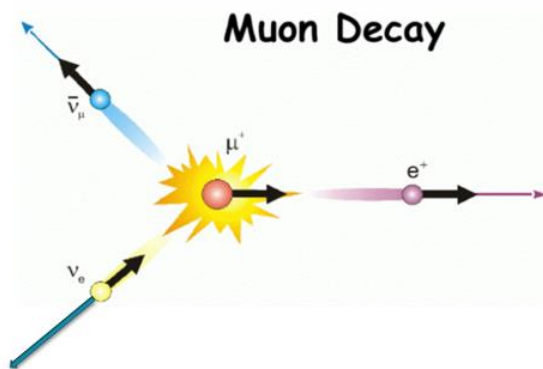


Figure 4. Muon decay at rest; black arrows are particles' spins, colored arrows are velocities



Muon within the Standard Model of Fundamental Particles

We can analyze the muon decay using the existing theory of the Standard Model of Fundamental Particles, which are all listed on Figure 5 below as consisting of six quarks (nuclear-type particles), six electron-like leptons, four force carriers (bosons) and the so-called Higgs boson (Schwartz, 2014). The current SM has been able to describe in a single mathematical pattern all visible matter in galaxies, which makes 4% of the mass of the Universe. It thus states that this matter consists of leptons and quarks making known nuclei and atoms and many unstable particles created in high-energy particle collisions. The remaining 96% of the Universe is made from a still mysterious set of “Dark Matter” and “Dark Energy”.

Figure 5.

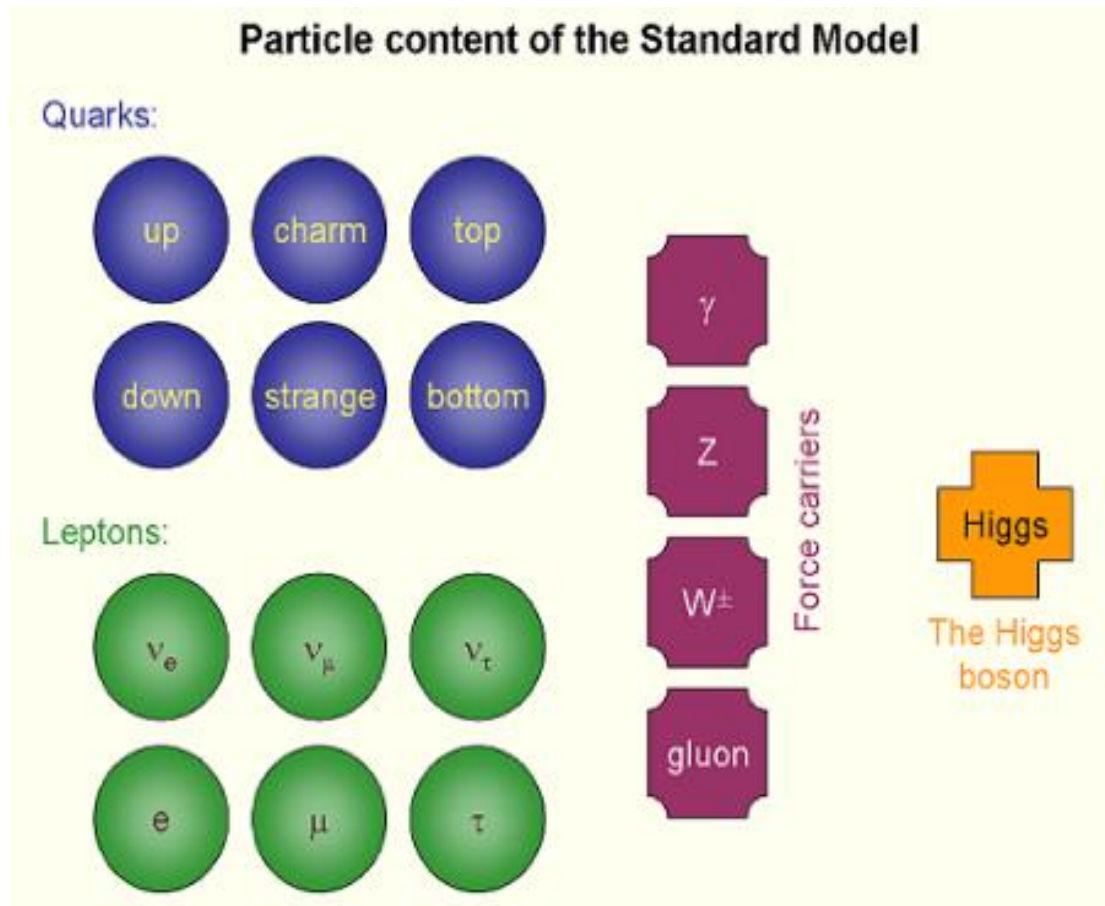
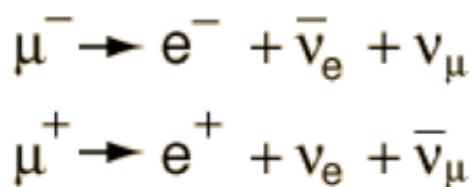


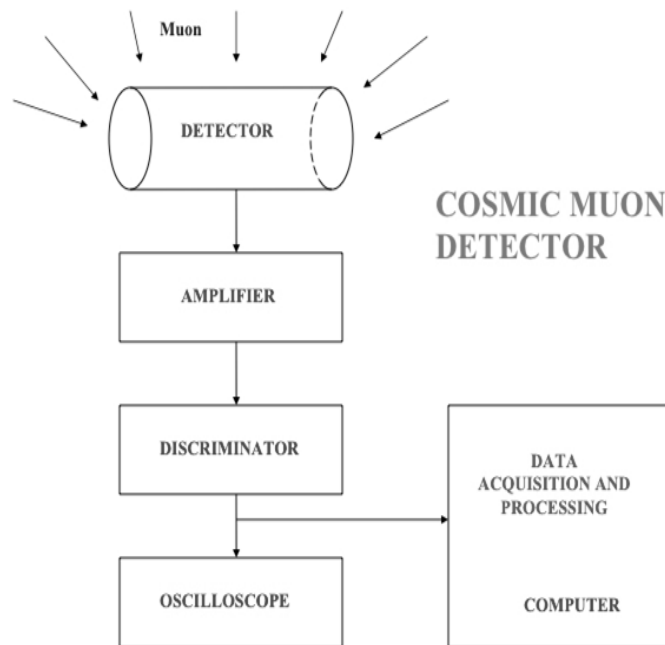
Figure 6. How muons decay; plus and minus superscripts denote the sign of the electric charge of muons and electrons, a bar above the neutrino symbol ν denotes an antineutrino.



Experimental set-up

Muons moving at speeds close to the speed of light enter, slow down, stop, and subsequently decay in the plastic scintillator detector. Each muon gives rise to two light-converted-to-voltage pulses separated by a few microseconds: one pulse when it enters the scintillator, and a second one when the muon decays. The pulses can be viewed with an oscilloscope or can be digitized and stored on the computer. We measure the time difference between these correlated pulses, as well as the amplitude of each pulse and the number of pulses in a given time. The voltage pulses are proportional to the particle energy loss in the detector. (Pierce, 2003).

Figure 7. Diagram of experimental setup.

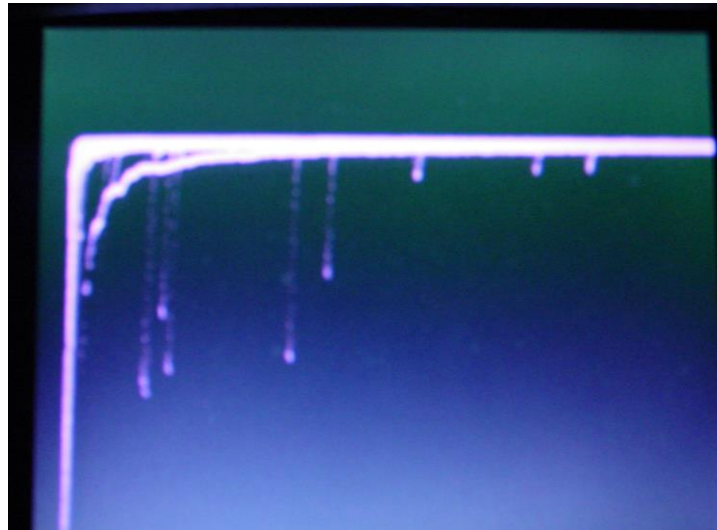


We recorded the muon decay events using both digital (computer) and analog (oscilloscope) methods.

Figure 8. In the image below, the black cylinder is our detector with the photomultiplier tube (PMT). The blue box is the high-voltage power supply with a control software, connected with an oscilloscope on top for an analog recording, or with a computer for digital processing.



Figure 9. The oscilloscope display shows large overlapping muon voltage pulses on the left and several smaller electron pulses to the right. The distance on the horizontal time axis between a muon and the corresponding electron pulse gives us directly the lifetime of the individual muon.



Details of our digital system

- Our apparatus is comprised of a single cylindrical plastic (mostly carbon) scintillator coupled to a 5" diameter PMT; its power supply voltage is set at 1060 volts; an ADC card PCI-DAS4020/1 sitting in the computer, with an associated data analysis software.
- The muon trigger is sent out only if the muon has decayed in the detector. The dead time marker was set to 230 nanoseconds (ns) in order not to have two triggers within that time, while the ramp reset time is set at 35 microseconds (μs): if a second (coincidence) event happens within this time, it is considered a muon decay event.
- Our detector stops and identifies - by their emitted electron - muons of kinetic energy below $E_{\text{max}} = 140 \text{ MeV}$ (megaelectronvolt $\text{MeV} = 1.60 \times 10^{-13}$ joules), as calculated from the stopping power of carbon of $2 \text{ MeV}/(\text{g}/\text{cm}^2)$ typical for relativistic (moving close to the speed of light) muons. Higher energy (up to 4 GeV, gigaelectronvolt $\text{GeV} = 1000 \text{ MeV}$) muons are just passing through our system, we counted them in a separate run. The detector has recorded huge numbers of unclassified cosmic ray events of arbitrary energy.

Data acquisition

- Due to low rate of low-energy cosmic muons at sea level and a small volume of the detector, to collect enough data we run the data acquisition each time for a period of about one week.
- We collected simultaneously muon decay times, fluxes of low-energy (stoppable) muons and energy spectra of muons and decay electrons/positrons in arbitrary units. In addition, we collected data on arbitrary high-energy particles passing through our detector.

Extraction of muon lifetime from our data

Our muons are electrically both positive and negative, with the accepted average ratio ρ of their numbers in the flux $\rho = N^+/N^- = 1.18 \pm .12$, which is due to the main initial cosmic ray particle – proton – being positive.

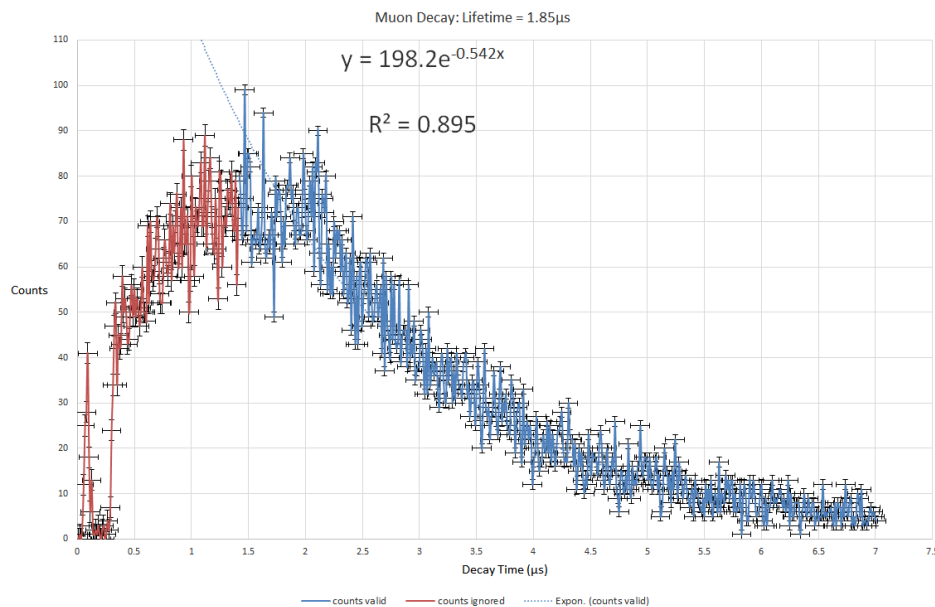
In a material negative muon, in addition to decaying, also disappear by muon capture in atomic nuclei, so their average lifetime τ^- there is shorter than the lifetime τ^+ of positive muons, which is the same as the free muon (positive or negative) lifetime τ_0 : $\tau^- < \tau^+ = \tau_0$. As a result, strictly speaking, the expected decay curve is a superposition of two exponentials plus a constant background term: $N=N_0(\rho e^{-t/\tau_0} + e^{-t/\tau^-}) + C$. (Reitner et al, 1960).

But instead of using a two-exponential fit, we found our experimental lifetime τ_{exp} as averaged between plus and minus muons, using a single-exponential fit, and extracted τ_0 later. (Coan, n.d).

The method

- Plot data as histogram
 - Fit with an exponential curve, possibly plus a constant
 - The curve is representing number N of muon decays after time t , after it stops in detector:
- $$N = N_0 e^{-\lambda t} + C, \text{ where } \lambda \text{ is the decay rate, } C \text{ is a background count; identify decay rate } \lambda.$$
- Take the inverse $\rightarrow \tau_{\text{exp}} = 1/\lambda$ - this is mean lifetime in matter, weighed between two kinds of muons.

Figure 10. A typical data trend curve without the background term C , with error bars shown



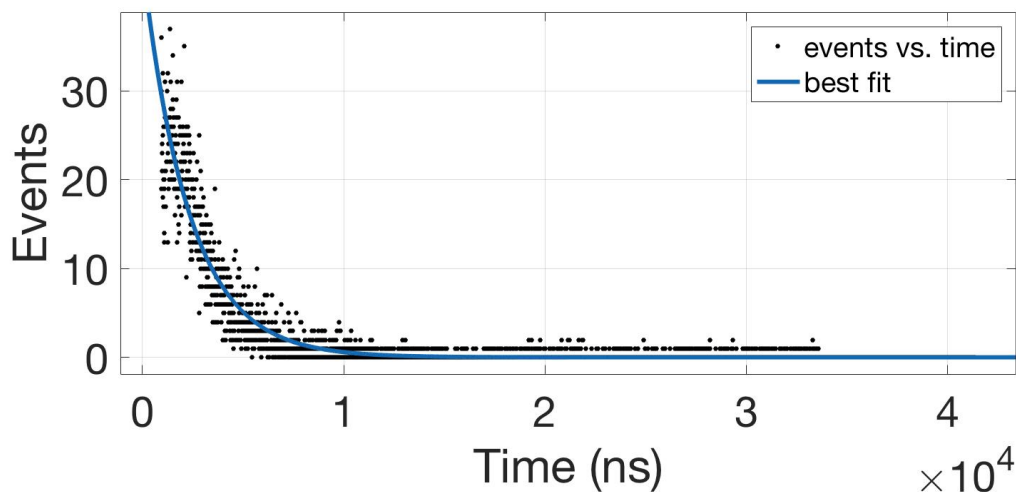
The lifetime of both muons in vacuum is related to our measured averaged lifetime τ_{exp} and to the known ratio ρ of numbers of positive and negative muons and the negative muon lifetime τ^- in carbon by the formula

Figure 11.

$$\tau_0 = \frac{\tau_{\text{exp}}}{(\rho + 1) \left(\tau_{\text{exp}} / \tau^- \right)}$$

Using the experimental negative muon lifetime in carbon-12: $\tau^- = 2.025 \pm 0.004 \mu\text{s}$, and $\rho = 1.18 \pm .12$, together with our experimental lifetime τ_{exp} , we received from our experiment the muon lifetime in empty space: $\tau_0(\text{this experiment}) = 2312 \pm 49 \text{ ns}$, which has 5.23% error with respect to the accepted value of $\tau_0 = 2197 \pm 0.04 \text{ ns}$.

Figure 12. Our experimental muon decay curve: exponential + constant



- Number of muon events: 6990
- Counting time: 1 week = 604800 s
- $\tau_0 = 2312 \pm 49 \text{ ns}$
- $C = 0.0263 \pm 0.0569$

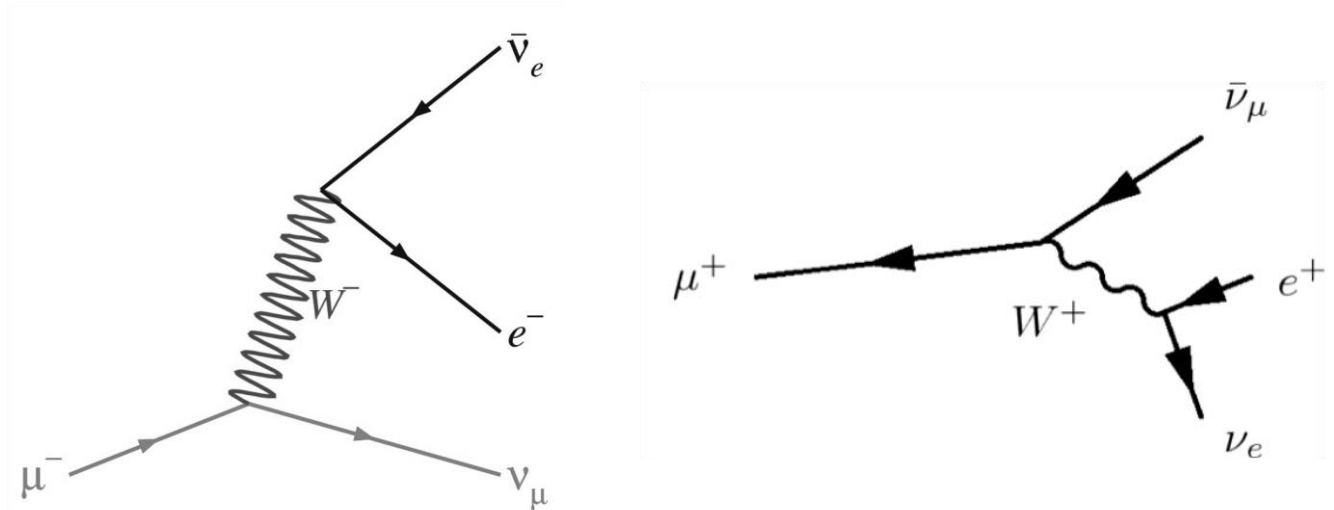
Standard Model implications from our lifetime value

In SM the well-known electromagnetic force is closely related to the “weak” interparticle force responsible for particles’ decays, such as the muon decay. The strength of this instability force in SM is denoted by g_w and it determines how long a muon exists before it breaks up.

The theoretical lifetime formula permits to find this so called weak coupling constant g_w .

As represented in the so-called Feynman diagrams below, muons (electrically positive or negative) decay through the intermediate emission of W bosons:

Figures 13 and 14



The muon lifetime formula for τ as calculated from these diagrams depends on g_w and on masses of W-boson M_W and muon m_μ ; it also depends on the speed of light c and the quantum Planck constant \hbar :

Figure 15 (Griffith, 2008)

$$\tau = \frac{1}{\Gamma} = \left(\frac{M_W}{m_\mu g_w} \right)^4 \frac{12\hbar(8\pi)^3}{m_\mu c^2}$$

Solving this formula for g_w , we have:

$$\text{Eq. (1)} \quad g_w = 8(3\pi \hbar / 2\tau m_\mu c)^{2/3} (M_W / m_\mu)$$

and using our measured lifetime τ_0 together with the experimental rest-mass energies of W-boson $M_W c^2 = 80.4 \text{ GeV}$ and of muon $m_\mu c^2 = 105.7 \text{ MeV}$, we have calculated one of the fundamental constants of nature - the dimensionless strength of the weak force g_w to be $g_w = 0.680$, with 4% error when compared with the accepted value of 0.653.

In SM, the electroweak force is mediated by the photon exchange, while the weak force is mediated by heavy bosons W^+ , W^- and Z^0 . Accordingly, the strengths of the electric force, given by the electric charge e , and of weak force, as given by g_w , must related by the SM formula (Quigg, 2013)

$$e = g_w \sin\theta_w \hbar c e$$

in which θ is an additional parameter (the “weak angle” of mixing photon with Z^0 boson), taken from other experiments, and ϵ_0 is the well-known electric permittivity of vacuum. When

we use our experimental value of g_w and take the accepted value $\theta=29^\circ$, we receive for the elementary electric charge the value $e = 1.85 \times 10^{-19}$ coulombs, to be compared with the textbook value of $e = 1.602 \times 10^{-19}$ coulombs, with an error of 7.27 %.

Higgs field vacuum density

According to SM, space is filled with the so-called Higgs field, undetectable by the experiments on relative motion of objects with respect to it. The existence of this field was finally confirmed in 2012 by the discovery of the particle of this field – the Higgs particle, the last particle predicted by SM many years ago.

It turns out that our measurement of the muon lifetime immediately permits to find the average density of the Higgs field, referred to as its vacuum expectation value v . The v is an important universal physical constant that factors into the mass formula of every fundamental particle. The degree to which a particle interacts with the Higgs field determines how massive the particle is. We calculated v from our calculated g_w , using the SM formula:

$$\text{Eq. (2)} \quad v = 2M_w c^2 / g_w \sqrt{\hbar c} = (2\pi m_\mu c^2 / 3\pi \hbar)^{1/4} (m_\mu c^2 / 4v\hbar c).$$

As can be seen here, v depends only on the muon lifetime and its mass. Using again $m_\mu c^2 = 105.7$ MeV and our value $g_w = 0.680$, we receive $v = 207$ GeV/ $\sqrt{\hbar c}$, to be compared with the accepted value of 246 GeV/ $\sqrt{\hbar c}$, with the percent error of 16% (Griffith, 2008).

Particle energy spectra

Each time a cosmic ray particle hits the detector, it releases energy. The detector then reports the energy of the particle, in proportion to its path length in the detector, as well as the energy of the emitted electron (in arbitrary units), tallying these events afterwards. We have graphed the muon kinetic energy lost in our detector (Figure 16) and electron (or positron) energy (Figure 17) of decay electrons.

Figure 16. Stopping muon kinetic energy lost in the detector; the spectrum ends at 140 MeV. Muons' deposited energy distribution is dictated by the geometry and orientation of our detector.

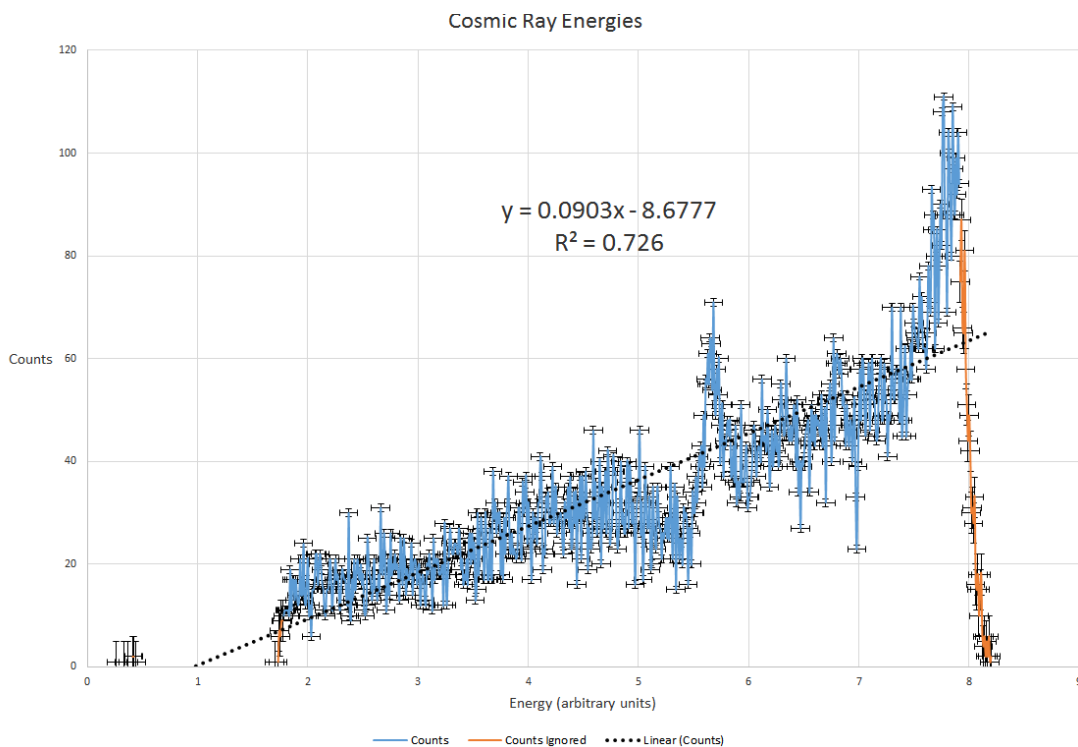
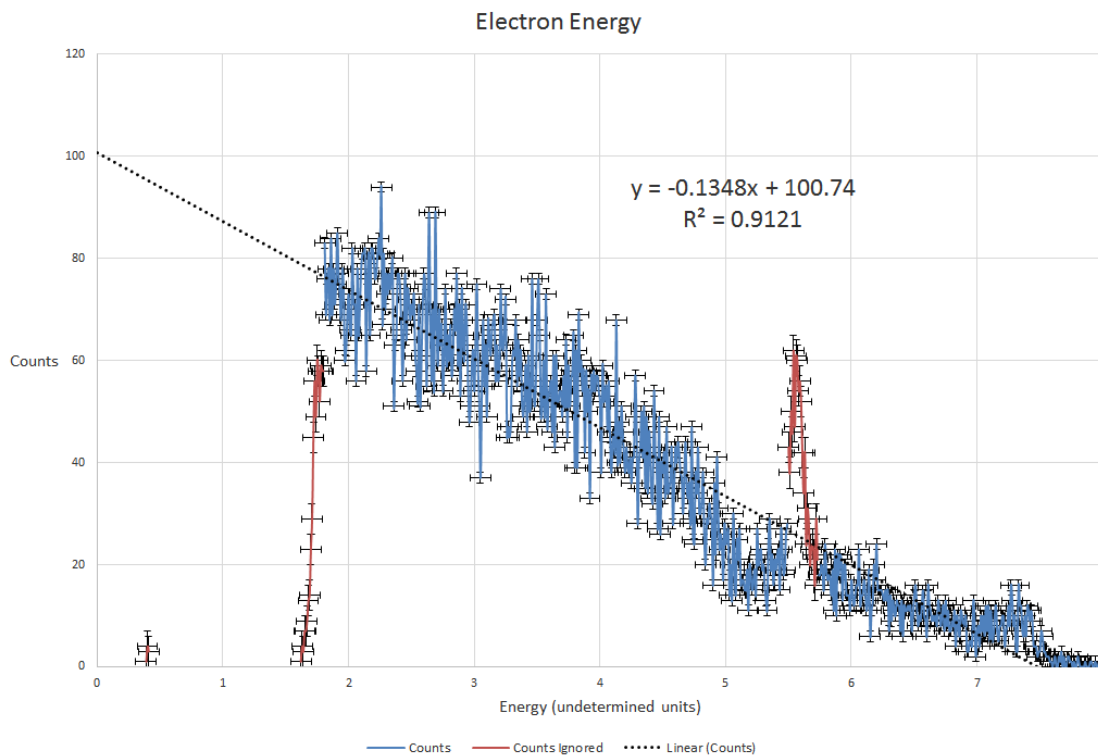


Figure 17. Electron/positron deposited energy spectrum, ends at 53 MeV.



Electron energy is the energy that the electron lost in detector before escaping outside. Electrons are created with energies from zero to a half of the muon rest-mass energy $m_{\mu} c^2 / 2 = 53 \text{ MeV}$.

For spatially uniform flux, more electrons are created around boundaries (there is more volume there, so more muons stop there), and they escape depositing only small amount of

their energy in the detector (short path in the detector): the observed spectrum is explained by the geometry of the experiment.

Muon flux below 140 MeV

The muon flux Φ is the number of muon events N_μ per unit area A per unit time T : $\Phi = (N_\mu/T)/A$.

This is a direction-averaged value, since isotropically arriving from space muons laterally travel through a thicker layer of atmosphere and many are absorbed there.

Our result for the flux of low-energy (below 140 MeV) muons is $\Phi = 0.78 \text{ muons/s} \cdot \text{m}^2$. Concentrating on low-energy muons which are stoppable in our detector, we have missed most of the muons, which are passing through our detector without stopping, because their energies are up to 4 GeV.

Day versus night muon flux

While it is known that, in addition to supernovae events, cosmic rays are also produced through solar activity, it is not established how significant of a source the sun is. By comparing muon flux during the day to night-time flux, when the Earth acts as a shield, we were able to determine whether or not there was a notable difference.

Our result of $\Phi_D/\Phi_N = 1.04 \pm 0.04$ indicates that there is virtually no statistical difference between day and night flux, and therefore that the sun is not a significant source of cosmic rays.

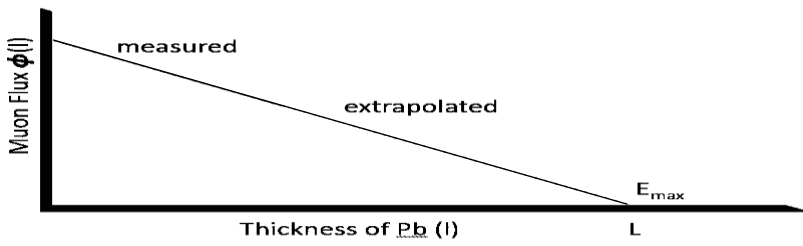
Lead Shielding of Atmospheric Muons

Figure 18. Our detector (black cylinder) is shielded from above with 10 cm layer of lead plates and bricks.



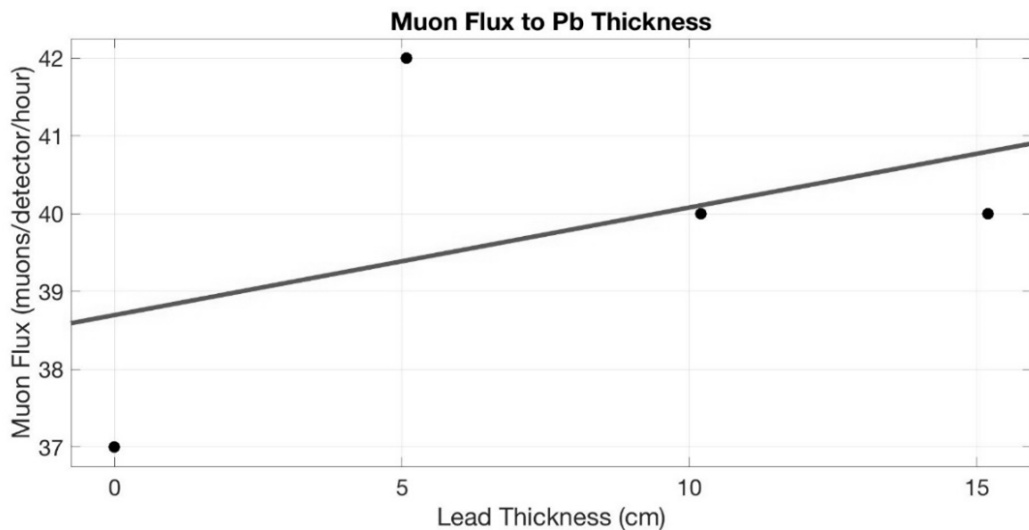
Our next goal was measuring average muon stopping power in lead, an important parameter in shielding from the cosmic rays. Stopping power in lead is the muon energy loss dE per unit path length dl in the muon-absorbing lead layer: dE/dl . It can be related to the muon flux's ϕ dependence on the thickness of the lead layer covering our detector, $\phi(l)$.

Figure 19. Expected muon absorption curve in lead



Then we could relate the slope $d\phi/dl$ of the flux curve (rate of muon absorption in lead) $\phi(l)$ to the stopping power: assuming for simplicity a linear decrease of muon flux with the increasing thickness of lead, eventually our most energetic muons at kinetic energy of $E_{max} = 140$ MeV should be stopped by some depth L of the Pb shield. Then from L we could find dE/dl as E_{max}/L . We do not have to achieve the full absorption of the most energetic stoppable muons: it would be sufficient to measure just the initial part of the absorption curve, and then to use instead of L its extrapolated value $L = \phi_0 / (d\phi/dl)$, where ϕ_0 is the muon flux with no lead shielding.

Figure 20. Stopping flux of low-energy muons/detector/hour vs lead shielding



Our results for four different lead layers of up to 15 cm in thickness for $\phi(l)$ are shown above, with the curve fit of $\phi=0.138l + 38.7$. The slope of the trend line is very flat, and with repeated trials we would likely see it becoming flatter. Instead of observing the expected flux attenuation in lead, we see a practically constant flux.

Explanation: Apparently in the flux there are muons more energetic than 140 MeV. While many muons originally below 140 MeV are captured by 10 and 15 cm of the lead shield, muons coming down from air with kinetic energies between 140 to 280 MeV are all slowed below 140 MeV and so are stopped and decay in the detector, replacing those absorbed in lead.

Conclusion 1: we have confirmed that there are atmospheric muons with energies both below and above 140 MeV.

Conclusion 2: incoming muon energy spectrum is flat at least up to 300 MeV, therefore more energetic muons slowed down by lead restore fully the lower-energy flux, absorbed in lead.

This is confirmed by the existing data: sea-level muons have energies up to 4 GeV, and their spectrum below 1 GeV is flat. We register only 3% of the total flux, by limiting ourselves to energies below 300 MeV.

Muon lifetime in the presence of the lead shielding

While measuring low-energy stoppable muon flux in the presence of the lead shielding, we also recorded the muon lifetime. Surprisingly, the presence of lead shielding has dropped the measured lifetime on average by 6.05%. Lead shielding, which only slows down muons, should not be changing the muon lifetime in material of detector.

Total muon flux of all muons passing through the detector

Rather than detecting only muons stopping in the detector, we separately measured spectrum and flux of all cosmic particles, presumably muons of any energy, stopping or passing through the detector. We recorded 375808 muons in 81789 s, giving us 5 muons/s/detector, or $\phi = 0.11 \mu/\text{cm}^2 \text{ min}$. The accepted value of the total sea-level muon flux: $1 \mu/\text{cm}^2 \text{ min}$ (L3 Collaboration, 2004). Apparently, our detector is missing a lot of high-energy muons.

We plan to measure the total flux with lead shielding, find a flux absorption curve of Fig. 19 and determine from it the stopping power of muons in lead dE/dl .

Significance of this research

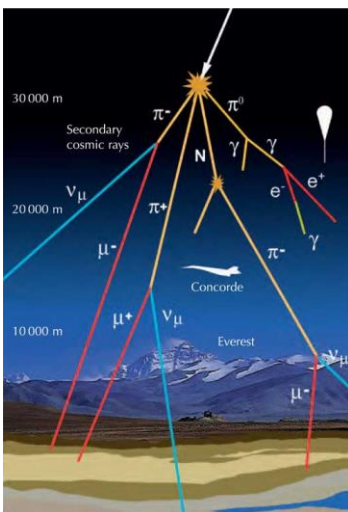


Figure 21.

This experiment meant to show that the first- and second-year students at community colleges can be doing experiments at the most fundamental level. Using high-energy cosmic ray particles available freely at the college physics lab, we can experiment with four of the 12 fundamental particles of nature: muon, electron, the muonic neutrino and the electronic neutrino (the last two both escaping undetected). Our calculations illustrate the interdependence of several fundamental constants within the Standard Model, as well as the importance of accurate μ lifetime measurements. Our results agree well with the accepted values.

Very surprising seems to be an ability to calculate elementary electric charge value from a seemingly completely unrelated, non-electric weak decay process. Equally surprising seems to be a chance to calculate the average energy of all-penetrating Higgs field, responsible for the masses of all twelve fundamental particles of matter and itself being the manifestation of the recently discovered Higgs boson. This shows how powerful the Standard Model is at explaining and relating thousands of elementary particle experiments. Because muon lifetime and its mass were known long before 1964, then the Higgs field energy density, expressible only in these two parameters, could have been easily calculated back in 1964, as soon as the Higgs field idea was developed by its six original authors as an explanation of why matter has mass.

We cannot explain our consistent results that the muon lifetime in the detector was depending on the thickness of the lead absorber on top of our detector, except for unaccounted for experimental errors.

Muon tomography: practical applications of cosmic-ray muons

Cosmic-ray muons were used to detect shielded nuclear materials being smuggled into the country, to produce images of the interiors of ancient structures, such as pyramids, and to study the internal structure of volcanoes. By comparing the ratio of the muon flux arriving from free space to that which arrives through the volcano, we can understand volcanic inner structure. Muons can be used to the same effect for detection of heavy radioactive material that x-rays are used for bone structure analysis. Historical structures, which we do not want to physically disturb to perform an analysis, can be similarly studied using this Muon Tomography.

References

1. PhysicsOpenLab (n.d.) *Cosmic Ray Muons & Muon Lifetime*
<http://physicsopenlab.org/2016/01/10/cosmic-muons-decay/> .
http://www.kayelaby.npl.co.uk/general_physics/2_7/2_7_7.html
2. Schwartz, M.D. (2014). *Quantum Field Theory and the Standard Model*. Cambridge University Press.
3. Pierce, Mark. (2003). *Measuring the Lifetime of Cosmic Ray Muons*.
<http://www-f9.ijs.si/~rok/sola/praktikum4/mioni/muonlab.pdf>
4. Reitner, R.A., et al. *Precise measurements of the mean lives of μ^+ and μ^- mesons in carbon*. Physical Review Letters, (1960), 5(1), pp. 22-23.
5. Coan, T.E., Ye, J. (n.d.). *Muon Physics*. Rutgers University report.

<http://www.physics.rutgers.edu/ugrad/389/muon/muonphysics.pdf>

6. Quigg, Chris. (2013). *Gauge Theories of the Strong, Weak and Electromagnetic Interactions*. Princeton University Press.

7. Griffith, David (2008). *Introduction to Elementary Particles*. Wiley-VCH Verlag.

8. L3 Collaboration, et al. *Measurement of the atmospheric muon spectrum from 20 to 3000 GeV*. Physics Letters B, (2004), 598 (1-2), pp. 15-32.

All accepted values not taken from sources above were found at the NIST database retrieved from: <http://physics.nist.gov>.

Image credits:

Figure 1.

Kliwer, S. *The Compact Cosmic Ray Telescope aboard the Kuiper Airborne Observatory*. Retrieved from http://cosmic.lbl.gov/SKliwer/Cosmic_Rays/Muons.htm

Figure 3.

Papadopoulos, L. (2014, November 20). *New Research Suggests Potential Link Between Neutrinos and the Supermassive Black Hole at Milky Way's Center*. Retrieved from <http://www.americaspace.com/2014/11/20/new-research-suggest-potential-link-between-neutrinos-and-the-supermassive-black-hole-at-milky-ways-center/>

Figure 4.

Brewer, J.H. (2004, March 26). *Introduction to Muon Spin Rotation*. Retrieved from <http://cmms.triumf.ca/intro/ppt/UNBC/Intro/img5.html>

Figure 5.

University of Glasgow, Department of Physics. *Particle Physics Theory*. Retrieved from <http://www.physics.gla.ac.uk/ppt/research.htm>

Figure 6.

(2017, May). *EWT (Electroweak theory)*. Retrieved from <http://cronodon.com/Atomic/EWT.html>

Figure 11.

Rutgers University, Department of Physics. (2009, January 5). *Muon Physics*. Retrieved from <http://www.physics.rutgers.edu/ugrad/389/muon/muonphysics.pdf>

Figure 13.

Pich, A. (2000, January 27). *Lessons learnt from the heavy tau lepton*. Retrieved from <http://cerncourier.com/cws/article/cern/28162>

Figure 14.

Ballett, P., Pascoli, S. (2012, September 12). *L-E_μ and the LENF*. Retrieved from <http://www.ippp.dur.ac.uk/~ballett/LENF/> and [hep-ph/1201.6299](http://arxiv.org/abs/hep-ph/1201.6299)

Figure 15.

Griffith, David (2008). *Introduction to Elementary Particles*. Wiley-VCH Verlag.

Figure 21.

Physics Open Lab (2016, January 10). *Cosmic Ray Muons & Muon Lifetime*. Retrieved from <http://physicsopenlab.org/2016/01/10/cosmic-muons-decay/>